

# Coordinated optimization scheduling operation of integrated energy system considering demand response and carbon trading mechanism

Peihong Yang<sup>a</sup>, Hui Jiang<sup>a,\*</sup>, Chunming Liu<sup>b</sup>, Lan Kang<sup>a</sup>, Chunling Wang<sup>b</sup>

<sup>a</sup> School of Information Engineering, Inner Mongolia University of Science and Technology, Baotou 014010, China

<sup>b</sup> School of Electrical and Electronic Engineering, North China Electric Power University, Beijing 102206, China

## ARTICLE INFO

### Keywords:

Integrated energy system  
Demand response  
Ladder-type carbon trading  
Optimize operation scheduling

## ABSTRACT

The low-carbon economy operation of the integrated energy system can be realized by introducing the demand response and carbon trading mechanism into the optimal scheduling of the integrated energy system. In this paper, an optimal scheduling model based on CCHP and carbon capture device is proposed, which takes into account the demand response of cooling, heating and electricity load and ladder-type carbon trading mechanism. Firstly, a multi-energy and multi-type demand response model based on time-of-use electricity price and incentive mechanism is established, and user satisfaction is used to evaluate it. Then, a carbon trading model of integrated energy system is established considering the actual carbon emissions of the system and the ladder-type carbon trading mechanism. Finally, taking the minimum sum of energy purchase cost, maintenance cost, carbon emission cost and compensation cost as the objective function, combined with the operation constraints of multi-energy flow of integrated energy system, an optimal scheduling model which takes into account both low-carbon and economy is constructed, and the problem is transformed into a mixed integer linear problem and solved by CPLEX. By setting up four scenarios for example analysis, the results show that the system total cost of the ladder-type carbon trading is decreased by 5.9% compared with the traditional carbon trading, and on the basis, the system total operating cost is decreased by 3.1% after considering the user-side DR. The simulation results further show that the introduction of DR and ladder-type carbon trading mechanism can flexibly transfer load, reduce gas purchase and reduce system carbon emissions, which has significant application value.

## 1. Introduction

With the increasingly serious crisis of traditional fossil energy and environmental pollution, the development of renewable energy has become an important means for governments to promote energy reform and build an environment-friendly society [1–2]. In recent years, in order to promote large-scale absorption of renewable energy and improve energy utilization, integrated energy systems (IES) have been vigorously promoted and applied [3]. Optimal scheduling is not only the premise of IES energy generation, energy utilization and the balance of supply and demand, but also the key to realize the coordination, complementarity and economic operation of many heterogeneous energy sources subsystems in IES [4–5].

As an important controllable resource in the operation of IES, demand response (DR) can realize the cooperative interaction between supply and demand of IES, stabilize the load peak and valley curve and promote the economic operation of energy system [6–7]. The common

demand response is only for electric loads, which can be divided into translatable, transferable and curtailable loads according to the characteristics of user-side load demand, and can also be divided into price-based DR (PBDR) and incentive-based DR (IBDR) according to the response form [8–9]. However, there are loads with different characteristics in IES, such as electricity, heat, cold, and gas load. Even the same type of load shows different response behaviors under different excitations. At the same time, there are complex coupling characteristics between multi-energy flows. For this reason, DR participation in IES optimization scheduling can provide more flexible adjustment potential [10]. Therefore, how to fully exploit the demand-side flexibility resources in the IES and study the optimal scheduling of the IES considering multi-energy and multi-type demand responses are of great significance.

At present, many researches have been carried out on the optimal scheduling of IES considering DR at home and abroad. Ref. [11] established a price-based integrated energy system DR model, using different electricity price schemes and interval probability to optimize the load

\* Corresponding author.

E-mail address: [jh\\_0321@126.com](mailto:jh_0321@126.com) (H. Jiang).

<https://doi.org/10.1016/j.ijepes.2022.108902>

Received 18 June 2022; Received in revised form 19 October 2022; Accepted 15 December 2022

Available online 23 December 2022

0142-0615/© 2022 The Author(s). Published by Elsevier Ltd. This is an open access article under the CC BY-NC-ND license (<http://creativecommons.org/licenses/by-nc-nd/4.0/>).

Nomenclature			
<i>Abbreviations</i>			
IES	Integrated energy system	$\mu$	Length of carbon emission interval
CCHP	Combined cooling heating and power	k	Carbon trading price increase rate
DR	Demand response	$\varphi$	Conversion coefficient of electric power into the thermal power
IDR	Integrated demand response	f	Cost
PBDR	Price-based demand response	$\varepsilon$	Reimbursement cost
IBDR	Incentive-based demand response	<i>Superscripts</i>	
CHP	Combined heat and power	t	Time
AC	Absorption chiller	chr	Charge to battery
PV	Photovoltaic	dis	Discharge from battery
WT	Wind turbine	ti	Transfer in load
MT	Micro gas turbine	to	Transfer out load
RHB	Recovery heat boiler	max	Maximum value
GB	Gas boiler	min	Minimum value
EH	Electric heating	E	Electrical load
EC	Electric cooling	H	Heat load
CC	Carbon capture	C	Cooling load
EES	Electric energy storage	<i>Subscripts</i>	
TES	Thermal energy storage	p	DR preload
CES	Cold energy storage	s	Shifting load
IGDT	Information gap decision theory	c	Cuttable load
MILP	Mixed integer linear programming	in	Indoor
<i>Parameters</i>		out	Outside
$\lambda_{PMV}$	PMV index	i	Conversion equipment
M	Human energy metabolic rate	<i>Other</i>	
I <sub>cl</sub>	Clothing heat resistance group	$\lambda_C$	Unit energy consumption coefficient
K	Building heat transfer coefficient	$\xi_C$	Share of CO <sub>2</sub> captured by carbon capture devices
F	Building surface area	$\theta_{gridbuy}$	Power purchase price
V	Building volume	$\theta_g$	Unit calorific value cost
c <sub>air</sub>	Indoor air specific heat capacity	$\theta_i^{pm}$	Equipment maintenance costs
$\rho_{air}$	Indoor air density	S	Satisfaction
$\kappa$	Weight coefficient	EC	Carbon capture volume
$\eta$	Efficiency	ECO <sub>2</sub>	Total CO <sub>2</sub> emissions
$\alpha$	Energy storage self-loss rate	$R_i^{down}$	Minimum climbing rate of l
$\beta$	Carbon emission coefficient	$R_i^{up}$	Maximum climbing rate of l
c	Carbon trading price	P <sub>gridbuy</sub>	Power purchase

curve, and combined with the optimal configuration of energy supply-equipment to complete the coordinated scheduling of the integrated energy system. Ref. [12] considered the DR of electric and heat loads on the user-side, which realized the real-time optimal scheduling operation of a high proportion of renewable energy connected to the IES. Ref. [13] constructed an IES coupled with electricity and gas, and realized the optimal distribution of electricity and natural gas supply and demand after the introduction of DR. Ref. [14] considered the electrical load PBDR in the combined heat and power (CHP) system. The example results show that the user transferred part of the electrical load during the peak period of electricity consumption, which not only relieves the power supply pressure of the system, but also improves the stability of the whole system. Ref. [15] considered the electrical load PBDR in CCHP, which effectively reduced the system operating cost. Ref. [16] constructed an energy hub framework and considered the electrical load PBDR to change the energy consumption of user electricity. IBDR means that the energy supplier signs a contract with user, in which the supplier can curtail off part of the user's load and give a certain compensation or electricity discount during the peak time of energy consumption. Ref. [17] introduced IBDR in the electro-thermal IES, and the results showed that a more economical and stable operation state of IES could be obtained without affecting user satisfaction. Ref. [18] considered IBDR in the optimal scheduling of cooling, heating and electrical IES,

which verified the effectiveness of DR in reducing randomness. However, the introduction of DR will have a certain impact on user satisfaction [19], and changes in electricity consumption behavior will cause user dissatisfaction and discomfort.

Under the double carbon goal, the optimization research of IES has also begun to transform from traditional economic scheduling to low-carbon economic scheduling. At present, there has been extensive research on the low-carbon economic scheduling of IES, which can be divided into two categories: one is to punish the environmental cost of carbon emissions generated by the system; the other is to trade carbon emissions generated by IES in the carbon trading market environment. Under the penalty of carbon emission cost, the use of carbon capture devices to capture carbon dioxide from coal-fired, gas-fired power plants has become a hotspot of IES research [20]. However, the carbon capture process will consume the electric energy of the power system, and the operation mode of the carbon capture device can be reasonably optimized through the electricity market to ensure the economic operation and reduce carbon emissions of the IES [21]. Ref. [22] combined carbon capture device with micro-turbine (MT) to reduce the carbon emissions of MT. Carbon trading costs are mainly determined by carbon allowance and carbon emissions. When the carbon emissions are greater than the carbon allowance, the carbon trading cost is positive, which means that the initial carbon allowance is insufficient and the insufficient part needs

to be purchased from the carbon market; on the contrary, the carbon trading cost is negative, and the excess can be sold to profit from the carbon market [23]. The introduction of carbon trading mechanism can effectively reduce the system carbon emissions and reduce the system operating cost [24]. Ref. [25] considered the traditional carbon trading mechanism in the electricity-gas IES and analyzed the impact of the formulation of carbon trading on system economy and carbon emissions. Ref. [26] analyzed the difference between the traditional carbon trading mechanism and the ladder-type carbon trading mechanism, verified the effectiveness of the ladder-type carbon trading mechanism in reducing carbon emissions, and provided a certain theoretical basis for the low-carbon economic operation of IES. Ref. [27] introduced a ladder-type carbon emission mechanism in the IES with DR of electrical, heating and gas loads and analyzed its low-carbon characteristics. The results show that the introduction of carbon trading mechanism can effectively reduce carbon emissions. Ref. [28] proposed a low-carbon economic scheduling model and operation strategy of CCHP integrated energy system, and analyzed the impact of carbon trading prices on low-carbon scheduling results. Ref. [29] comprehensively considered the information gap decision theory (IGDT) and the ladder-type carbon trading mechanism, and established a multi-objective optimal scheduling model, which can effectively reduce carbon emissions while ensuring the economic operation of the IES.

The above literatures are all single research on DR or ladder-type carbon trading mechanism, but with the in-depth research on IES optimization operation, domestic and foreign scholars have noticed that the introduction of a single DR and ladder-type carbon trading mechanism is limited in the ability of IES to optimize operation. The integrated application of DR and carbon trading technology can improve its optimal scheduling ability. Ref. [30] studied the optimal scheduling scheme based on the combination of carbon trading mechanism and electricity load DR, and the results show that the combination of the two can further reduce carbon emissions and system operating costs. To further review the research status of optimal scheduling of IES considering DR and carbon trading mechanisms, a brief summary is given in Table 1.

According to the above literature research, there are few studies on the optimal scheduling of IES considering both DR and ladder-type carbon trading mechanisms, and only electricity load is considered even if DR is considered. For this reason, this paper proposes to study the optimal scheduling operation of the IES that comprehensively considers the DR of cooling, heating and electric load and the ladder-type carbon trading mechanism. The main contributions are as follows:

- 1) An IES optimal operation scheduling model based on CCHP, carbon capture, cooling, heating and electric load DR and ladder-type carbon trading mechanism is constructed.
- 2) Under the demand response operation scheme of cooling, heating

and electricity load, the comprehensive satisfaction index of cooling, heating and power load is proposed, and the impact of DR on the low-carbon economic operation of the IES is deeply analyzed.

3) This paper proposes a carbon allowance mechanism in line with the operating characteristics of IES and constructs a ladder-type carbon transaction cost model, which can reduce system carbon emissions and achieve low-carbon operation of IES economy.

The remainder is organized as follows. In Section 2, the IES model with DR and carbon capture device is established, and the DR model of electric, heating and cooling loads are constructed; In Section 3, the model of ladder-type carbon trading mechanism is constructed; In Section 4, the IES optimization operation scheduling model is established, including the objective function, power balance and constraints. In Section 5, an example is analyzed in four different scenarios to verify the effectiveness of the model; Section 6 addresses the conclusion of the study.

## 2. Structure analysis and model of IES with DR and carbon capture device

### 2.1. IES structure

IES can promote the coupling of cold, heat, electricity and gas to realize the cooperative and optimal operation of multi-energy systems and meet the multi-energy needs of users. In this paper, an IES structure diagram with DR and carbon capture devices, as shown in Fig. 1. The IES constructed in this paper is connected to the upper-level power grid and gas network, and it can purchase energy from the upper-level energy network to satisfy the energy demand of users. In addition to getting energy directly from upper-level energy network, the system is also equipped with wind turbine (WT) and photovoltaic (PV) to decrease carbon emissions while reducing energy purchase costs. Energy-coupling equipment includes micro gas turbine (MT), gas boiler (GB), recovery heating boiler (RHB), absorption chiller (AC), electric heating (EH) and electric chiller (EC), which can realize energy flow between networks. Energy-storage equipment includes electric energy storage (EES), thermal energy storage (TES) and cold energy storage (CES). The introduction of energy-storage equipment can promote energy consumption and enhance the flexibility of the system. Load-side includes electricity, cooling and heating loads. On this basis, the introduction of DR can not only smooth the fluctuation of load curve, but also reduce the operating cost of the system.

### 2.2. DR model

DR means that users adjust their energy use habits according to load price or incentive mechanism, which can participate in power grid

**Table 1**  
Summarization of literature review.

Reference	PBDR (Electric load)	IBDR (Electric load)	IBDR (Heat load)	IBDR (Cooling load)	Traditional carbon trading	Ladder-type carbon trading
[11]	√	×	×	×	×	×
[12]	√	√	×	×	×	×
[13]	√	×	×	×	×	×
[14]	√	×	×	×	×	×
[15]	√	×	×	×	×	×
[16]	√	×	×	×	×	×
[17]	√	√	√	√	×	×
[18]	√	√	×	×	×	×
[25]	×	×	×	×	√	√
[26]	×	√	×	×	√	√
[27]	√	×	×	×	×	√
[28]	×	×	×	×	×	√
[29]	√	√	×	×	√	√
[30]	√	√	×	×	×	√
Current paper	√	√	√	√	√	√

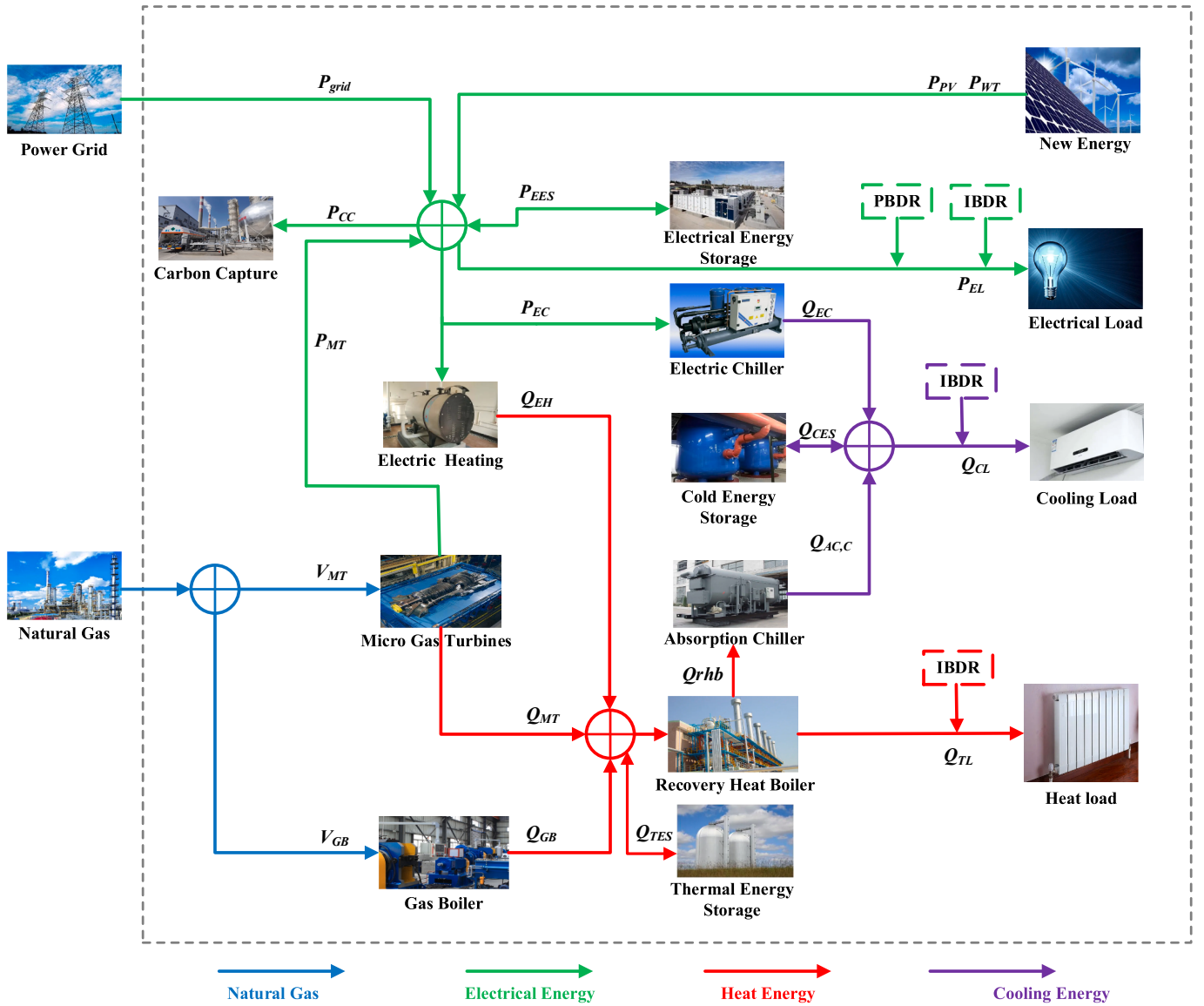


Fig. 1. IES structure diagram with DR and carbon capture device.

interaction, optimize load curve and improve system stability. DR can be divided into price-based demand response (PBDR) and incentive-based demand response (IBDR) according to its response form. The traditional demand-side load response mostly only considers the electricity load DR, but the cooling and heating load is similar to the electric load, which has the potential to implement DR scheduling. Considering the coupling characteristics of heterogeneous load, this paper constructs DR models for electricity, heating and cooling load respectively. In addition, it also comprehensively considers the satisfaction index of electricity consumption and the comfort of heating and cooling load, and takes it as an evaluation standard to analyze the level of user satisfaction after the implementation of DR.

### 1) Electricity load DR model

Electricity load can be divided into fixed electricity load and flexible electricity load. The flexible electrical load can be divided into transferable load and curtailable load according to the DR characteristics. The transferable load can balance the supply and demand of the system through DR scheduling, and the transferable load is 0 during the whole scheduling cycle. The curtailable load means that the supplier curtails part of the power to a certain extent and gives some compensation in order to alleviate the power supply pressure. The electrical load DR

model are as follows:

$$\begin{cases} P_e^t = P_{p,e}^t + P_{s,e}^t - P_{c,e}^t \\ P_{s,e}^{\min,t} \leq P_{s,e}^t \leq P_{s,e}^{\max,t} \\ \sum_{t=1}^T P_{s,e}^t = 0 \\ 0 \leq P_{c,e}^t \leq P_{c,e}^{\max,t} \end{cases} \quad (1)$$

where  $P_{p,e}^t$  and  $P_{s,e}^t$  are the electricity loads before and after the DR at time  $t$ , respectively;  $P_{c,e}^t$  is the electricity load after participating in the DR that can be curtailed at time  $t$ ;  $P_{s,e}^{\min,t}$  and  $P_{s,e}^{\max,t}$  are the minimum and maximum value for transferable electricity load at time  $t$ , respectively, which is 15 % of the total load;  $P_{c,e}^{\max,t}$  is the maximum value for curtailable electricity load at time  $t$ , which is 10 % of the total load.

The satisfaction index of electrical load can be described as [31]:

$$S_e = \left(1 - \frac{P'_{c,e}}{P'_{p,e}}\right) \cdot 100\% \quad (2)$$

where  $S_e$  is the satisfaction index of electrical load.

2) Heating load DR.

When the indoor temperature fluctuates within a certain range, it does not affect the user's thermal comfort, referred to as the user's perception of the heat load temperature has ambiguity. Therefore, the predicted mean vote (PMV) [32] index is introduced to quantitatively represent the thermal comfort of users. The PMV calculation formula is:

$$\lambda_{PMV} = 2.43 - \frac{3.76(T_s - T_{in}^t)}{M(I_{cl} + 0.1)} \quad (3)$$

where  $M$  is the human energy metabolic rate, generally taken as 80 W/m<sup>2</sup>;  $I_{cl}$  is the clothing heat resistant group, generally taken as 0.11(m<sup>2</sup> °C)/W;  $T_s$  is the average temperature of human skin in a comfortable state, generally taken as 33.5°C;  $T_{in}^t$  is the indoor temperature at time  $t$ .

Considering that PMV can effectively improve the flexible adjustment ability of temperature load, users are active frequently during the daytime, their thermal perception ability is more sensitive and their comfort requirements are high compared to night. The variation range of PMV in the whole scheduling cycle is as follows:

$$\begin{cases} |\lambda_{PMV}| \leq 0.9, t \in [1:00 - 7:00] \cup [20:00 - 24:00] \\ \lambda_{PMV} \leq 0.5, t \in [8:00 - 19:00] \end{cases} \quad (4)$$

The heating load demand is closely related to the indoor and outdoor temperatures, and the requirements for indoor temperature vary with real-time changes in outdoor temperature and the type of load point. According to the characteristics of indoor and outdoor temperature and thermodynamic changes, the transient thermal balance equation between heat load demand and temperature is [33]:

$$\frac{dT_{in}^t}{dt} = \frac{P_H - (T_{in}^t - T_{out}^t)KF}{c_{air}\rho_{air}V} \quad (5)$$

where  $T_{out}^t$  is the outdoor temperature at time  $t$ ;  $K$ ,  $F$  and  $V$  are heat transfer coefficient, surface area and volume of buildings, respectively;  $c_{air}$  and  $\rho_{air}$  is the specific heat capacity and density of indoor air, respectively;

Existing studies have proved that the heterogeneous load IDR mechanism considering different forms of cooling, heating and electric is effective and practical. The heat load DR is similar to the electric load, which is adjustable in time and space. Therefore, the heat load has both transferable load and curtailable load, and the DR model of the heat load are as follows:

$$\begin{cases} P'_h = P'_{p,h} + P'_{s,h} - P'_{c,h} \\ P'_{s,h}{}^{\min,t} \leq |P'_{s,h}| \leq P'_{s,h}{}^{\max,t} \\ \sum_{t=1}^T P'_{s,h} = 0 \\ 0 \leq P'_{c,h} \leq P'_{c,h}{}^{\max,t} \end{cases} \quad (6)$$

where  $P'_{p,h}$  and  $P'_{h}$  are the heating loads before and after the DR at time  $t$ , respectively;  $P'_{s,h}$  is the heating load after participating in the DR that can be transferred at time  $t$ , in which the transfer-in period is positive and the transfer-out is negative;  $P'_{c,h}$  is the heating load after participating in the DR that can be curtailed at time  $t$ ;  $P'_{s,h}{}^{\min,t}$  and  $P'_{s,h}{}^{\max,t}$  are the minimum and maximum value for transferable heating load at time  $t$ , respectively, which is 15 % of the total load;  $P'_{c,h}{}^{\max,t}$  is the maximum value for curtailable heating load at time  $t$ , which is 10 % of the total load.

The satisfaction index of heating load can be described as:

$$S_h = \left(T_s - T_{out,t} - \frac{M(2.43 - \lambda_{PMV})(R_c + 0.1)}{3.76}\right) \frac{KF}{P'_{p,h}} \cdot 100\% \quad (7)$$

where  $S_c$  is the satisfaction index of heating load.

3) Cooling load DR.

Similar to the heating load characteristics, the fluctuation of indoor temperature within a certain range will not affect the user's cooling experience. Users' perception of the comfort of the cold environment is also ambiguous, and the cooling load demand and indoor temperature satisfy the first order ordinary differential equation [34], which can be described as:

$$\frac{d\zeta_{in}^t}{dt} = \frac{1}{CR} (\zeta_{out}^t - \zeta_{in}^t - RP'_{p,c}) \quad (8)$$

where  $\zeta_{in}^t$  and  $\zeta_{out}^t$  are the indoor and outdoor temperatures at time  $t$ , respectively;  $C$  and  $R$  are the ambient equivalent thermal capacity and equivalent thermal resistance, respectively.

Similarly, the DR model of cooling load are as follows:

$$\begin{cases} P'_c = P'_{p,c} + P'_{s,c} - P'_{c,c} \\ P'_{s,c}{}^{\min,t} \leq |P'_{s,c}| \leq P'_{s,c}{}^{\max,t} \\ \sum_{t=1}^T P'_{s,c} = 0 \\ 0 \leq P'_{c,c} \leq P'_{c,c}{}^{\max,t} \end{cases} \quad (9)$$

where  $P'_{p,c}$  and  $P'_c$  are the cooling loads before and after the DR at time  $t$ , respectively;  $P'_{s,c}$  is the cooling load after participating in the DR that can be transferred at time  $t$ , in which the transfer-in period is positive and the transfer-out is negative;  $P'_{c,c}$  is the cooling load after participating in the DR that can be curtailed at time  $t$ ;  $P'_{s,c}{}^{\min,t}$  and  $P'_{s,c}{}^{\max,t}$  are the minimum and maximum value for transferable cooling load at time  $t$ , respectively, which is 15 % of the total load;  $P'_{c,c}{}^{\max,t}$  is the maximum value for curtailable cooling load at time  $t$ , which is 10 % of the total load.

The satisfaction index of cooling load can be described as:

$$S_c = \frac{\left(\frac{(\zeta_{out}^t - \zeta_{in}^t)}{R} - \frac{d\zeta_{in}^t}{dt} C\right) - P'_{c,c}}{P'_c} \cdot 100\% \quad (10)$$

where  $S_c$  is the satisfaction index of cooling load.

4) Comprehensive satisfaction of users.

In order to achieve the unified evaluation of the user satisfaction of electric, heating and cooling loads, this paper proposes a comprehensive satisfaction index to avoid the decline of user satisfaction caused by the over-response of the system. The model are as follows:

$$\begin{cases} S_{user} = \kappa_1 S_e + \kappa_2 S_h + \kappa_3 S_c \\ \kappa_1 + \kappa_2 + \kappa_3 = 1 \\ S_{user}^{\min} \leq S_{user} \leq 1 \end{cases} \quad (11)$$

where  $S_{user}$  is the comprehensive satisfaction of users;  $\kappa_1$ ,  $\kappa_2$  and  $\kappa_3$  are the satisfaction weight coefficients of electricity, heating and cooling load, respectively;  $S_{user}^{\min}$  is the minimum value of users' comprehensive satisfaction.

### 3. Ladder-type carbon trading mechanism

Carbon trading is to buy or sell carbon emissions rights as a commodity in the carbon trading market. The introduction of carbon trading mechanism can stimulate the response of energy supply enterprises to energy saving and emission reduction to a certain extent, and effectively reduce carbon emissions. Government regulators set carbon emission

rules for enterprise and issue free carbon emission allowances. When the carbon emission of the enterprise is lower than the free carbon emission allowances, the enterprise obtains additional income through the sale of the remaining carbon emission allowances in the carbon trading market, otherwise the enterprise need to purchase additional carbon emission allowances. Above carbon trading mechanism model primarily includes three elements: initial carbon allowance, actual carbon emissions and carbon trading costs.

### 3.1. Initial carbon allowance model

Before implementing carbon trading, carbon emission allowances must first be determined. At present, there are two common carbon emission allowance allocation methods in China: free allocation and paid allocation. Free allocation means that the regulator issuer free carbon emission allowances to increase the enthusiasm of enterprises for low-carbon emission reduction; paid allocation requires enterprises to pay corresponding fees for their own carbon emissions. At present, China uses free allocation and based on the baseline method to provide carbon emission allowance for the system [35], and the initial free carbon emission allowance is related to the actual power generation of the network. For the IES constructed with DR in this paper, the carbon emission sources are MT and GB. MT generates both power and heat, while GB produces only heat. Carbon emission allowance is allocated according to the total equivalent calorific value. Therefore, the free carbon emission allocation model of carbon trading are as follows:

$$\begin{cases} E^* = E_{MT}^* + E_{GB}^* \\ E_{MT}^* = \beta_h (\varphi \sum_{i=1}^T P_{MT}^{E,i,t} + \sum_{i=1}^T P_{MT}^{H,i,t}) \\ E_{GB}^* = \beta_h \sum_{i=1}^T P_{GB}^t \end{cases} \quad (12)$$

where  $E^*$  is the total allocation allowance of free carbon emission rights for the system, this paper stipulates that during the whole scheduling cycle,  $E^*$  takes 300 kg and the daily carbon allowance is cleared to 0 and cannot be accumulated;  $E_{MT}^*$  and  $E_{GB}^*$  are free carbon emission right allowance for MT and GB, respectively;  $\beta_h$  is the allocation of free carbon emission right allowance per unit heating power;  $P_{MT}^{E,i,t}$ ,  $P_{MT}^{H,i,t}$  and  $P_{GB}^t$  are the MT output electric power, MT output heating power and GB output heating power at time  $t$ , respectively;  $\varphi$  is the conversion coefficient of electric power into thermal power.

### 3.2. Actual carbon emission model

In this paper, the IES considers the carbon capture device, which will absorb part of the CO<sub>2</sub> in the process of operation. Therefore, when calculating the actual carbon emissions of IES, we should not only consider the carbon emissions generated by the above MT and GB, but also further consider the capture and absorption of CO<sub>2</sub> by carbon capture device. The equivalent output power of carbon capture unit consists of two parts: net output power and capture power consumption, in which capture power consumption is used to capture CO<sub>2</sub>, including operation power consumption and maintenance power consumption. In this paper, the carbon capture unit mainly captures the CO<sub>2</sub> produced during the operation of MT and GB in the system, and its model [36] are as follows:

$$\begin{cases} P_{Ei}^t = P_{Ni}^t + P_{Ci}^t \\ P_{Ci}^t = P_{si}^t + P_m^t \\ P_{si}^t = \lambda_C E_C^t \\ E_C^t = \eta_C \xi_C E_{CO_2}^t \\ E_{CO_2}^t = \eta_C^{MT} P_{MT}^t + \eta_C^{GB} P_{GB}^t \end{cases} \quad (13)$$

where  $P_{Ei}^t$  is the equivalent output power of the carbon capture device at time  $t$ ;  $P_{Ni}^t$  is the net output power of carbon capture device at time  $t$ ;  $P_{Ci}^t$  is the capture power consumption of the carbon capture device at time  $t$ ;  $P_{si}^t$  is the operating power consumption of the carbon capture device at time  $t$ ;  $P_m^t$  is the maintenance power consumption of the carbon capture device at time  $t$ , which is independent of the operation status of the carbon capture unit and can be regarded as a constant;  $\lambda_C$  is the power consumption coefficient of carbon capture device for capturing unit CO<sub>2</sub>;  $E_C^t$  is the carbon capture amount at time  $t$ ;  $\eta_C$  is carbon capture efficiency;  $\xi_C$  is the percentage of CO<sub>2</sub> captured by the carbon capture device;  $E_{CO_2}^t$  is the total CO<sub>2</sub> emission of the system at time  $t$ ;  $\eta_C^{MT}$  and  $\eta_C^{GB}$  are the CO<sub>2</sub> emission conversion coefficient of MT and GB, respectively.

The actual carbon emission model of IES is:

$$E = E_{CO_2} - E_C \quad (14)$$

### 3.3. Carbon trading cost model

In this paper, based on the conventional carbon trading mechanism, a reward and punishment ladder-type carbon transaction cost calculation model [29] is constructed to further reduce carbon emissions according to the relationship between actual carbon emissions and free carbon allowances, and its model is shown in Fig. 2.  $c$  is the carbon trading price;  $\mu$  is the interval length of carbon emissions;  $k$  is the rate of increase in carbon trading price. In order to effectively reduce the actual emissions of CO<sub>2</sub>, the model divides the difference between the actual carbon emissions and the free carbon allowance into several sub-intervals, and the corresponding carbon trading prices are different in each interval. When  $f_{CO_2}^t$  is negative, it means that the actual carbon emission of the IES is lower than the free allocated carbon allowance, the IES obtains additional income through the sale of the allowance; when  $f_{CO_2}^t$  is positive, it means that the actual carbon emission for the IES is higher than the free allocated carbon allowance, the IES needs to purchase additional carbon allowance. The larger the difference between the actual carbon emissions and the free carbon allowances, the higher the carbon trading price. In summary, the calculation model of carbon trading cost  $f_{CO_2}^t$  is:

$$f_{CO_2}^t = \begin{cases} -c\mu - \delta(1+k)(E^* - E - \mu) & E - E^* \leq -\mu \\ -c(E^* - E) - \mu & -\mu \leq E - E^* < 0 \\ c(E - E^*) & 0 \leq E - E^* < \mu \\ c\mu + c(1+k)(E - E^* - \mu) & \mu \leq E - E^* < 2\mu \\ c\mu(2+k) + c(1+2k)(E - E^* - 2\mu) & 2\mu \leq E - E^* < 3\mu \\ c\mu(3+3k) + c(1+3k)(E - E^* - 3\mu) & 3\mu \leq E - E^* < 4\mu \\ c\mu(4+6k) + c(1+4k)(E - E^* - 4\mu) & 4\mu \leq E - E^* \end{cases} \quad (15)$$

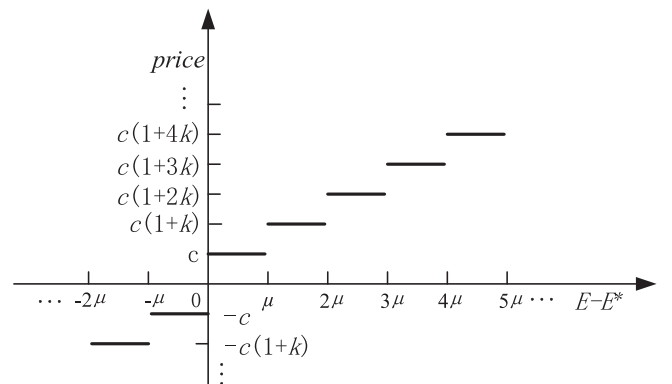


Fig. 2. Schematic diagram of ladder-type carbon trading mechanism.

#### 4. IES economic operation optimization model with DR and ladder-type carbon trading

##### 4.1. Objective function

The IES optimal operation model considering DR and ladder-type carbon trading aims to minimize the total operating cost of the system under the condition of meeting system constraints. The system total operating cost  $f$  in IES is minimized, including the energy purchase cost  $f_{buy}$ , the maintenance cost  $f_{om}$ , the carbon trading cost of  $f_{CO_2}$  and the compensation cost  $f_{DR}$ .

$$\min f = f_{buy} + f_{om} + f_{CO_2} + f_{DR} \quad (16)$$

##### 1) Energy purchase cost

$$f_{buy} = \sum_{t=1}^T \theta_{gridbuy}^t P_{gridbuy}^t + \theta_g \sum_{t=1}^T [P_{MT}^t + P_{GB}^t] \quad (17)$$

where  $\theta_{gridbuy}^t$  and  $P_{gridbuy}^t$  are the unit price of electricity purchased and the power purchased at time  $t$ , respectively;  $\theta_g$  is the unit calorific value cost of gas consumed by MT and GB, which is 0.35¥ / kWh.

##### 2) Maintenance cost

$$f_{om} = \sum_{t=1}^T \sum_{i=1}^8 \theta_i^{om} P_i^t \quad (18)$$

where  $i$  takes 1, 2, ..., 8, respectively representing PV, WT, MT, GB, RHB, EC, EH and AC;  $\theta_i^{om}$  is the maintenance cost coefficient of equipment  $i$ ;  $P_i^t$  is the output power of the equipment  $i$  at time  $t$ .

##### 3) Carbon trading cost.

$$f_{CO_2} = \sum_{t=1}^T f_{CO_2}^t \quad (19)$$

##### 4) Compensation cost

$$f_{DR} = \sum_{t=1}^T [\varepsilon_{c,e} P_{c,e}^t + \varepsilon_{c,h} P_{c,h}^t + \varepsilon_{c,c} P_{c,c}^t] \quad (20)$$

where  $\varepsilon_{c,e}$ ,  $\varepsilon_{c,h}$  and  $\varepsilon_{c,c}$  are compensation cost coefficients for curtailment of electrical, heating and cooling loads.

#### 4.2. Constrains

##### 4.2.1. Renewable energy output constraint

$$\begin{cases} 0 \leq P_{PV}^t \leq P_{PV}^{\max} \\ 0 \leq P_{WT}^t \leq P_{WT}^{\max} \end{cases} \quad (21)$$

where  $P_{PV}^t$  and  $P_{WT}^t$  are the PV and WT active power output at time  $t$ , respectively;  $P_{PV}^{\max}$  and  $P_{WT}^{\max}$  are the upper limit of PV and WT active power output, respectively.

##### 4.2.2. MT and GB operation constraints

$$\begin{cases} P_q^t = \eta_q L_{HVNG} P_{q,g}^t \\ P_q^{\min} \leq P_q^t \leq P_q^{\max} \\ -R_q^{down} \Delta t < P_q^{out,t+1} - P_q^{out,t} < R_q^{up} \Delta t \end{cases} \quad (22)$$

where  $q$  is MT and GB, respectively;  $P_q^t$  and  $P_{q,g}^t$  are the output power of  $q$  and the natural gas consumption power of  $q$  at time  $t$ , respectively;  $\eta_q$  is the conversion efficiency of  $q$ ;  $L_{HVNG}$  is the calorific value of natural gas;  $P_q^{\min}$  and  $P_q^{\max}$  are the upper and lower limits of  $q$  output power, respectively;  $R_q^{down}$  and  $R_q^{up}$  are the upper and lower limits of  $q$  climbing rate, respectively.

##### 4.2.3. Operation constraint of energy-coupling equipment

The energy coupling-equipment includes AC, EH, EC, RHB and so on. Such devices enable the interconversion of different energies, such as heat to cold, electric to cold, electric to cold, etc., which only involves the conversion coefficient, so a unified formula can be used for model.

$$\begin{cases} P_w^{out,t} = \eta_w P_w^{in,t} \\ P_w^{\min} \leq P_w^{out,t} \leq P_w^{\max} \end{cases} \quad (23)$$

where  $w$  is AC, EH, EC and RHB, respectively;  $P_w^{in,t}$  and  $P_w^{out,t}$  are the input and output power of energy-coupling equipment  $w$  at time  $t$ , respectively;  $\eta_w$  is the energy conversion coefficient of energy-coupling equipment  $w$ ;  $P_w^{\max}$  and  $P_w^{\min}$  are the upper and lower limits of energy-coupling equipment  $w$  output power, respectively.

##### 4.2.4. Energy-storage equipment operation constraint

The introduction of electric, thermal and cold energy storage devices can further improve the operation flexibility of the system. Since the three energy storage equipment have similar operating characteristics, a unified formulation can be used to model [37].

$$U_{ES,n}^t = \begin{cases} (1 - \alpha) U_{ES,n}^{t-1} + (P_{ES,n}^{chr,t} \Delta t) \\ (1 - \alpha) U_{ES,n}^{t-1} - (P_{ES,n}^{dis,t} \Delta t) \end{cases} \quad (24)$$

$$\begin{cases} U_{ES,n}^{\min} \leq U_{ES,n}^t \leq U_{ES,n}^{\max} \\ -P_{ES,n}^{chr,max} < P_{ES,n}^t < P_{ES,n}^{dis,max} \\ U_{ES,n}^0 = U_{ES,n}^T \end{cases} \quad (25)$$

where  $n$  is EES, TES, CES respectively;  $U_{ES,n}^t$  and  $U_{ES,n}^{t-1}$  are the capacity of  $n$  at time  $t$  and time  $t-1$ , respectively;  $\alpha$  is the self-loss rate of energy storage equipment  $n$ ;  $P_{ES,n}^{chr,t}$  and  $P_{ES,n}^{dis,t}$  are the charging and discharging power of energy storage equipment  $n$  at time  $t$ , respectively;  $\eta_{ES,n}^{chr}$  and  $\eta_{ES,n}^{dis}$  are the charging and discharging efficiencies of energy storage equipment  $n$ ;  $\Delta t$  is the charging and discharging time, taken as 1 h;  $U_{ES,n}^{\min}$  and  $U_{ES,n}^{\max}$  are the minimum and maximum energy storage capacity of energy storage equipment  $n$ , respectively;  $P_{ES,n}^{chr,max}$  and  $P_{ES,n}^{dis,max}$  are the maximum charge and discharge power of energy storage equipment  $n$ , respectively.

##### 4.2.5. Power balance constraint

$$\begin{cases} P_{gridbuy}^t = P_{EC}^t + P_{EH}^t + P_{CC}^t + P_{EES}^{chr,t} + P_e^t - P_{PV}^t - P_{WT}^t - P_{CHP}^t - P_{TES}^{dis,t} \\ H_{CHP}^t + P_{GB}^t + P_{EH}^t + P_{TES}^{dis,t} = P_{TES}^{chr,t} + P_h^t \\ P_{AC}^t + P_{EC}^t + P_{CES}^{dis,t} = P_{CES}^{chr,t} + P_c^t \\ 0 \leq P_{gridbuy}^t \leq P_{gridbuy}^{\max,t} \end{cases} \quad (26)$$

where  $P_{EES}^{chr,t}$  and  $P_{EES}^{dis,t}$  are the charging and discharging power of electric energy storage at time  $t$ , respectively;  $P_{gridbuy}^{\max,t}$  is the upper limit of purchasing power from the grid;  $P_{TES}^{chr,t}$  and  $P_{TES}^{dis,t}$  are the charging and discharging power of thermal energy storage at time  $t$ , respectively;  $P_{CES}^{chr,t}$  and  $P_{CES}^{dis,t}$  are the charging and discharging power of cold energy storage at time  $t$ , respectively.

#### 4.3. Model solving method

The solution of the IES optimal scheduling model based on DR and ladder-type carbon trading mechanism established in this paper is a mathematical programming problem considering constraints. In this

paper, the constraint conditions are linear constraints, so the solution model belongs to the mixed integer linear programming (MILP) problem. The CPLEX solver can be called in MATLAB to solve the optimization model and get the optimal operation result. The computer hardware environment is Intel (R) Core (TM) i5-6200U CPU, main frequency 2.30 GHz, memory 8.00 GB, and the software environment is Windows 10 system. The standard form of the solving model is equation (27), and the solving process is shown in Fig. 3.

$$\begin{cases} \min c^T x \\ \text{s.t. } A_{ineq} x \leq b_{ineq} \\ A_{eq} x = b_{eq} \\ x_{\min} \leq x_i \leq x_{\max}, i \in I \\ x_j \in \{0, 1\}, j \in J \end{cases} \quad (27)$$

where the optimization variable  $x$  includes the output of energy-supply equipment, the output of energy-coupling equipment, the output of energy-storage device, and the power purchase of power grid; Equality constraints include the energy balance equation of the system and the balance equation of the energy-storage equipment. Inequality constraints include the output of each equipment in the system.

## 5. Example analysis

### 5.1. Basic data

In order to verify the advantages of IES optimized operation model considering DR and ladder-type carbon trading mechanism in terms of economy and reducing carbon emissions, optimization calculation is

carried out based on the cooling, heating and electricity load data of a typical day in a place in China and the renewable energy forecast data. The scheduling period is 24 h a day and 1 h as the step. Fig. 4 shows the forecast data of renewable energy output, electricity load, heating load, and cooling load. The parameters of energy-supply equipment and energy-coupling equipment in IES system are shown in Table 2, the parameters of energy-storage equipment are shown in Table 3 [38], and the time of use pricing in peak, flat and valley periods are shown in Table 4 [39].

The natural gas price is taken as 3.45 ¥/m<sup>3</sup>, which is converted into a unit calorific value price of 0.35 ¥/kWh. The carbon emission conversion coefficients of MT and GB are both 0.98 kg/kWh. The carbon trading base price  $c$  is 0.3 ¥/kg, the carbon emission interval length  $\mu$  is 80 kg, and the carbon trading price growth rate  $k$  is 2/3. The upper limit of electricity purchased by IES from the grid is 300 kW. The compensation costs for curtailing electricity, heating and cooling loads are 0.7, 0.65 and 0.54 ¥/kWh, respectively.

### 5.2. Operation cost analysis of different scheduling models

In order to verify that the introduction of cooling, heating and electricity load DR and ladder-type carbon trading mechanism can reduce the cost of economic operation of the optimization model proposed in this paper, four different scenarios are set up to analyze, as shown in Table 5.

By calculating the above four scenarios, the each operating cost of system is shown in Table 6.

#### 1) Comparative analysis of Scenario 1 and Scenario 2.

As can be seen from Table 6, the total cost of scenario 1 is up to 7504.52 ¥. Because it does not consider DR and ladder-type carbon trading in the system for coordinated operation, which lacks flexibility. Compared with Scenario 1, Scenario 2 takes into account the DR of the user-side, users can flexibly change their energy habits according to the price signal or incentive mechanism, which can further reduce the pressure of energy-supply equipment. Therefore, compared to Scenario 1, the total operation cost decreased by 2.38 %.

#### 2) Comparative analysis of Scenario 1 and Scenario 3.

Compared to Scenario 1, Scenario 3 takes into account the ladder-type carbon trading mechanism. And compared to the Scenario 1, the gas purchases decreased by 9.1 %, which reduces the carbon emissions of the system. As can be seen from Table 6, compared to Scenario 1, the total operation cost decreased by 5.9 %.

#### 3) Comparative analysis of Scenario 3 and Scenario 4.

Compared with Scenario 3, Scenario 4 takes into account the user-side DR. On the basis of ladder-type carbon trading mechanism, the introduction of DR can achieve a reasonable scheduling arrangement and effectively reduce the operating cost of the system. As can be seen from Table 6, compared to Scenario 3, the total operation cost decreased by 3.1 %.

In summary, the introduction of ladder-type carbon trading mechanism has certain advantages in reducing IES carbon emissions, while the introduction of DR can reasonably schedule the equipment of the system, which can effectively reduce the operating cost of the system. Therefore, the scheduling strategy in this paper can achieve both economic and environmental win-win. The scheduling results of Scenario 4 are used to analyse the equipment output, DR analysis, customer satisfaction analysis and carbon emission analysis of each step of the IES system.

### 5.3. System equipment output analysis

After considering the DR and ladder-type carbon trading mechanism, the equipment output of the electric, heating and cooling loads are shown in Figs. 5-7. It can be seen from Fig. 5 that the electricity load demand is lower, the renewable energy output is sufficient and the

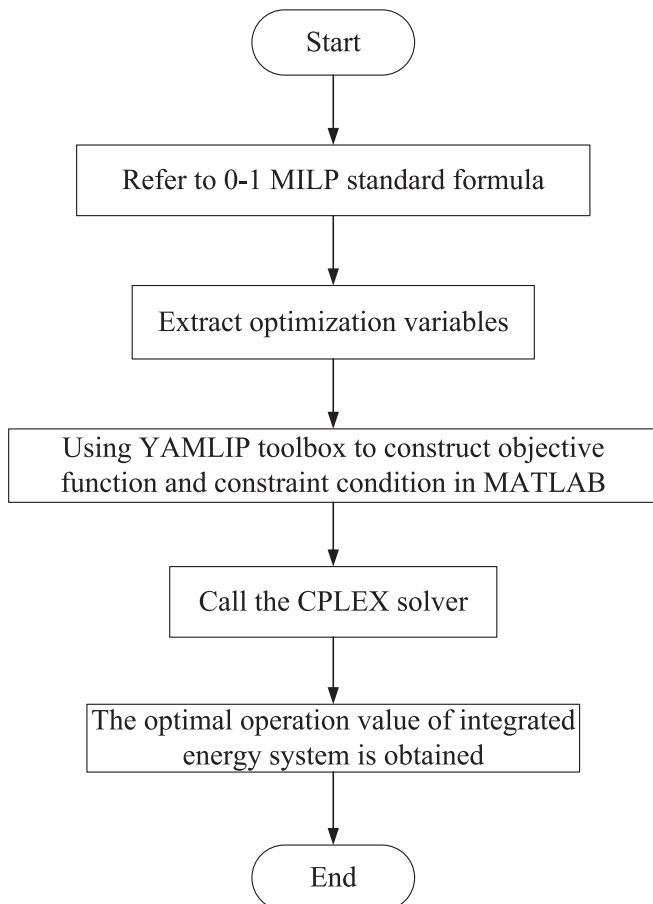


Fig. 3. Model solving process.

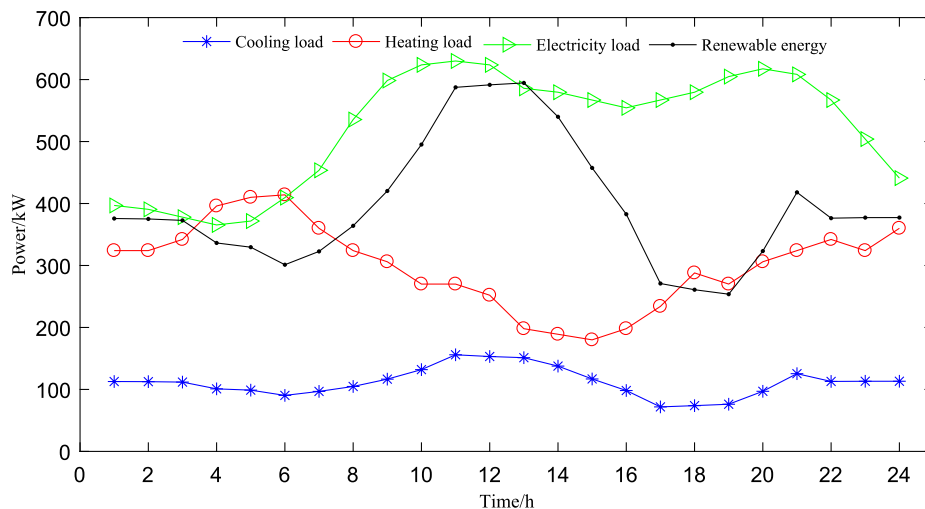


Fig. 4. Renewable energy output forecast and multi-energy load profiles of a typical day.

Table 2  
System equipment parameters.

Equipment	Operation and maintenance cost ¥/ kWh	Efficiency	Lower limit of output/ kW	Upper limit of output/ kW
PV	0.01	/	0	400
WT	0.01	/	0	500
MT	0.1	0.35	50	500
GB	0.05	0.85	0	500
WHB	0.2	1	0	300
EC	0.02	1.2	0	300
EH	0.02	0.99	0	300
AC	0.3	1	0	300

Table 3  
Energy-storage equipment parameters.

Parameters	EES	TES	CES
Charge and discharge efficiency	0.9	0.9	0.9
Self-loss rate	0.001	0.01	0.01
Upper limit of charge and discharge power/kW	90	60	120
Energy storage capacity/kWh	300	180	360
Lower limit of energy storage state	0.2	0.1	0.2
Upper limit of energy storage state	0.8	0.9	0.8
Operation and maintenance cost ¥/kWh	0.02	0.02	0.02

Table 4  
TOU electricity price.

Category	Time/h	Unit price ¥/ kWh
Peak tariff	8:00–11:00	0.804
	18:00–21:00	
Parity tariff	6:00–7:00	0.550
Valley tariff	12:00–17:00	0.295
	22:00–5:00	

Table 5  
Different scenario settings.

Scenario	Traditional carbon trading	DR	Ladder-type carbon trading
1	✓		
2	✓	✓	
3			✓
4		✓	✓

Note: ✓ indicates that this factor is taken into account.

Table 6  
System operation costs.

¥	Scenario 1	Scenario 2	Scenario 3	Scenario 4
$f_1/¥$	2059.1	2081.3	2059.1	2028
$f_2/¥$	2336.6	2043.2	2124.7	2030.3
$f_3/¥$	1630.62	1428.48	1515.4	1432.9
$f_4/¥$	1478.2	854.6	1365.9	800.9
$f_5/¥$	0	918.3	0	552.7
$f/¥$	7504.52	7325.88	7065.1	6844.8

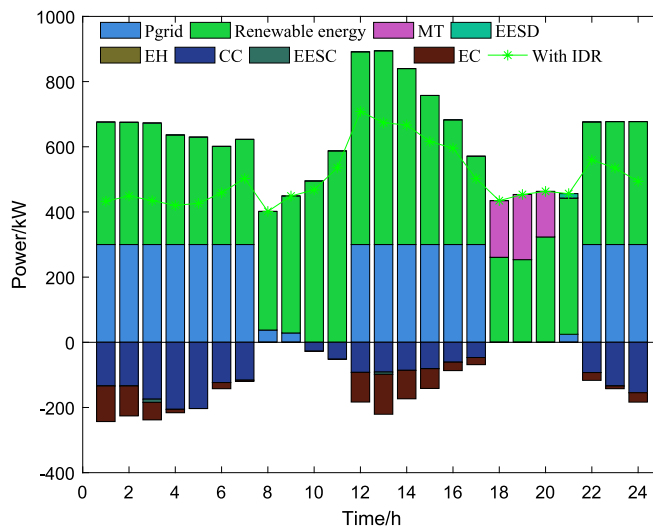


Fig. 5. Electric load equipment output.

electricity price is lower during the periods of 22:00–7:00 and 12:00–17:00, so the electricity load is mainly provided by electricity purchase and renewable energy during this period. In addition to meeting user demand, in order to fully absorb renewable energy and reduce the operating cost of the system, the excess electricity is supplied to other electrical equipment or stored in batteries. The electricity demand increases and the electricity price is at the peak during the periods of 8:00–11:00 and 18:00–21:00, the electricity is mainly provided by new energy in order to reduce the economic cost. Since the output of the PV unit is 0 from 18:00–20:00, the gas turbine starts to output in order to relieve the power supply pressure. At 21:00, the wind resource is sufficient and the battery is discharged. On the basis of meeting the user's

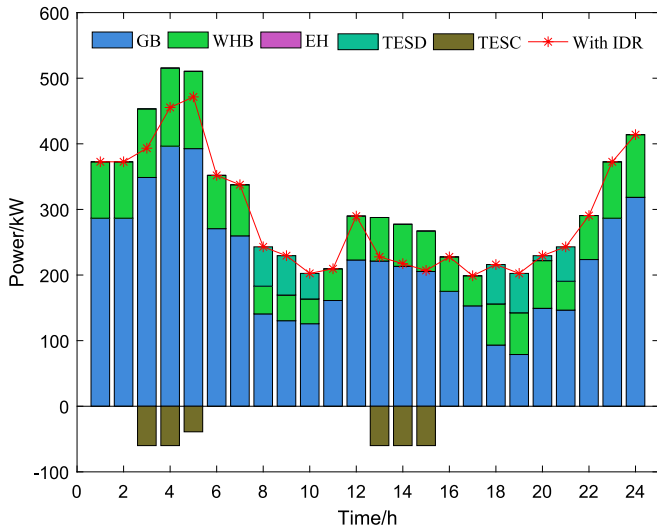


Fig. 6. Heating load equipment output.

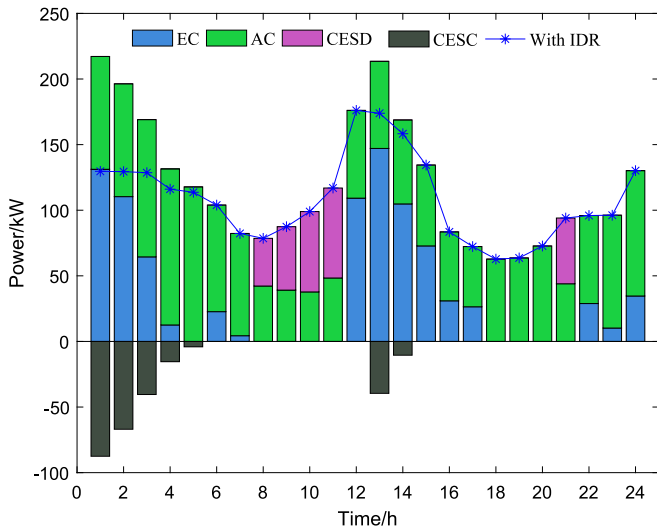


Fig. 7. Cooling load equipment output.

demand, in order to reduce carbon dioxide emissions, the output of the gas turbine is 0. The battery releases electric energy during the peak hour and charges during the period of sufficient electricity to ensure the economic and stable operation of the system.

As can be seen from Fig. 6, the heat load supply mainly depends on GB and RHB. The GB has more output during the period from 22:00–7:00, and the excess heat energy is stored in the TES on the premise of meeting the demands of users; The output of GB decreased from 8:00–17:00, as the heat demand began to decrease and the light was sufficient; 18:00–21:00 the MT began to output, as the demand for heat load began to increase and the output of GB was insufficient to meet the needs of users. The TES can store heat when the heat load is sufficient and release heat during the peak period of heat load, which can maintain the stability of the system. Although the EH is considered in the IES, the EH does not output under the condition of meeting the heat load demand and minimizing the economic cost.

As can be seen from Fig. 7, the cooling load is mainly provided by AC and EC. During the periods of 8:00–11:00 and 18:00–21:00, cooling load demand increases gradually and electricity price is high, power-supply equipment gives priority to providing electricity load for users, so this period mainly depends on AC to provide cold energy. In other periods, the EC as a supplement to the insufficient output of the AC, the output of

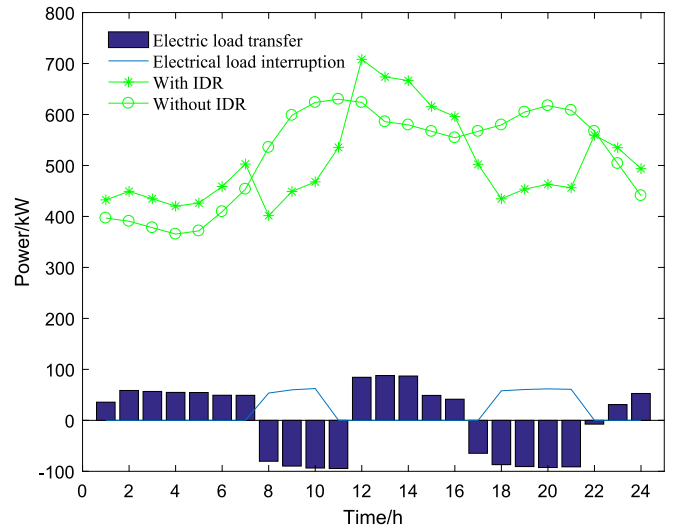


Fig. 8. Electricity load DR.

the EC is larger in the period of non-peak electricity price and more output of new energy, while meeting the cooling load demand of the system, store the excess cold energy in the CES. The CES releases the cooling load during the peak cooling periods or when the system is undersupplied, which can relieve the cooling pressure and maintain the stable operation of the system.

#### 5.4. Demand response analysis of electricity, heating and cooling load

Figs. 8-10 show the demand curves of users' electricity, heating and cooling loads before and after DR, as well as the load transfer and curtailment in each period. It can be seen from the figures that users actively participate in DR operation under the incentives of time of use tariffs and compensation costs. It can be seen from Fig. 8, the load after DR has a clear peak-to-valley distribution compared to that before DR. In order to alleviate the power supply pressure during peak period and maintain the system stability, the transferable load transfers some loads from peak tariff periods (08:00–11:00 and 18:00–21:00) to flat tariff periods and valley tariff periods, which reduces the peak tariff period load and increases the load of other electricity price periods. And the renewable output is larger during the valley tariff period, which not only fully consumes the renewable energy, but also reduces the system operation cost. Under the condition that the maximum curtailment constraint is met, the user makes load curtailment during the peak tariff periods (08:00–11:00 and 18:00–21:00), which further relieves the power supply pressure and reduces environmental pollution on the basis of transferable load.

As can be seen from Fig. 9, although 23:00–5:00 before the DR is in the peak period of heat consumption, GB and RHB produce more heat at this period, and there is a surplus load in addition to meeting user demand. Therefore, more transferable loads are transferred to this period to alleviate the heating pressure in other periods and maintain the stability of the system. During the periods of 6:00–11:00 and 17:00–22:00, GB and RHB produce less heat, which is not enough to meet the demands of users. On the basis of transferring part of the load, part of the load is curtailed to further alleviate the heating pressure and reduce the carbon emissions of the system.

As can be seen from Fig. 10, because the electricity price is in the valley and flat stage during 24:00–6:00 and 12:00–15:00, and the renewable energy output is larger, so there is excess electricity allocated to EC and the AC output is more in this period, which makes more transferable load to be used in this period. 7:00–11:00 and 16:00–23:00 are basically only the AC in operation, the cooling load generated is not enough to meet the demands of users. In order to alleviate the cooling

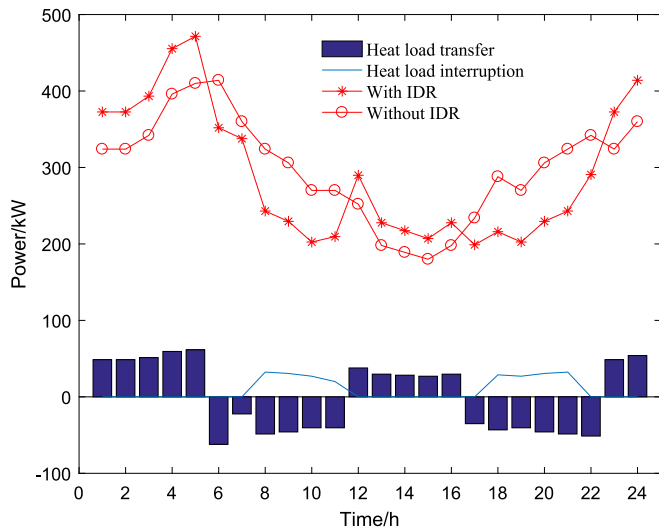


Fig. 9. Heating load DR.

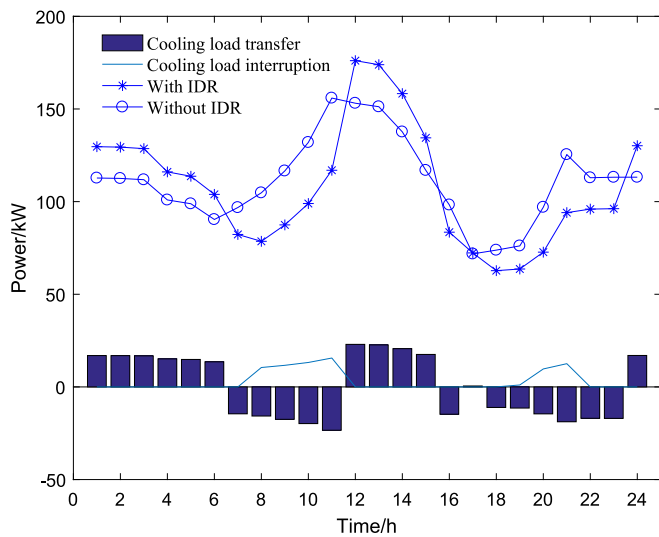


Fig. 10. Cooling load DR.

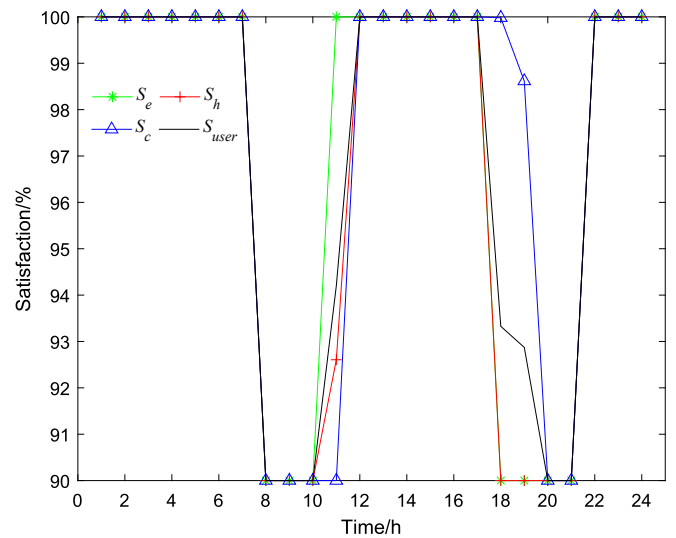


Fig. 11. Users' satisfaction.

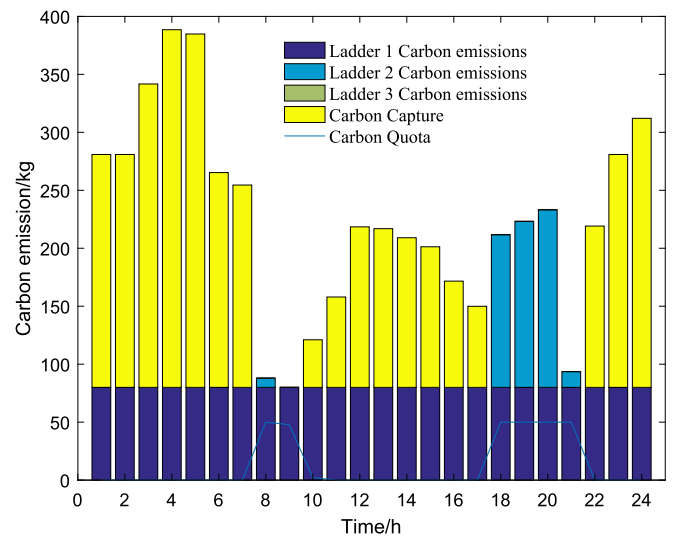


Fig. 12. Ladder-type carbon emissions.

pressure, and then reduce part of the load on the basis of transferring part of the load.

### 5.5. Analysis of users' satisfaction

The users' satisfaction is shown in Fig. 11. Electric load satisfaction is 90 % only at 8:00–11:00 and 18:00–21:00, and 100 % in other periods. Because of the high electricity consumption and high electricity price in these two periods, the system supply–demand balance has to be met by cutting some of the electrical load. The heating and cooling loads are similar to the electric loads, and the satisfaction is below 100 % in both time periods. Because of the high energy consumption and low energy production in these two time periods, the supply pressure is relieved by load curtailment. And because the comprehensive satisfaction index is the concentrated embodiment of cooling, heating and electric load satisfaction, the comprehensive satisfaction of users after considering DR is more than 90 %, and the overall satisfaction level is high. 08:00–11:00 and 18:00–21:00 are the peak periods of energy use, DR curtails part of the load to alleviate the pressure of energy supply and meet the supply–demand balance of the system, but it reduces the comprehensive satisfaction of users. In other periods, the load

curtailment power is 0, so the comprehensive satisfaction is 100 %. In summary, load curtailment power is negatively correlated with users' satisfaction, and the higher the curtailment power, the lower the users' satisfaction. Comprehensive satisfaction directly affects the enthusiasm of customers to participate in DR, and it can be used as a constraint to flexibly guide the load to participate in system optimization as well as to further improve the system operation economy.

### 5.6. Ladder-type carbon emissions analysis

As can be seen from Fig. 12, after the introduction of ladder-type carbon trading mechanism, the carbon emissions of ladder 3 are all 0 in the whole scheduling cycle. It can be verified that the actual carbon emissions of the system are reduced after the introduction of the ladder-type carbon emission mechanism, which not only realizes the low-carbon operation of the system, but also reduces the operating cost of the system. From 8:00–10:00 and 18:00–21:00, the demand for electricity is large, the electricity price is at the peak and the supply of renewable energy is insufficient, which leads to the operation cost of carbon capture being higher than the carbon emission cost of the ladder 2. Therefore, considering the economical operation cost, the carbon

capture device does not work at this time, and the carbon capture amount is 0. In the period of high carbon emissions, the carbon allowances are freely allocated, which can reduce carbon transaction costs and make the system operating costs lower.

## 6. Conclusion

Aiming at the problem of optimal operation of IES, this paper takes the minimum operating cost of the system as the objective function. Considering the compensation cost in DR and ladder-type carbon trading cost, an IES optimization operation model based on DR and ladder-type carbon trading mechanism is established to optimize the output of each equipment in the system. Through simulation verification, the following conclusions are drawn:

- (1) The proposed electric, heating and cooling load DR can effectively alleviate the energy supply pressure of energy supply equipment during the peak period of energy use. DR can flexibly adjust the user-side load, and at the peak period of energy use, it can curtail or transfer part of the load to maintain the stability of the system and reduce the operating cost of the system.
- (2) Under the incentive of time-of-use electricity price and compensation cost, users participate in DR spontaneously and have a high level of comprehensive energy satisfaction. The comprehensive satisfaction is only between 90 % and 100 % in the period of load curtailment, and 100 % in other periods. It is proved that there is a negative correlation between load power curtailment and comprehensive satisfaction.
- (3) The introduction of ladder-type carbon trading mechanism has greatly reduced carbon dioxide emissions. In the whole scheduling cycle, the carbon emissions of the ladder 3 are all 0, and there are only a few periods of carbon emissions in the ladder 2. And compared with the scenario without considering the ladder-type carbon trading mechanism, the system operating cost of the proposed strategy is decreased by 5.9 %, and the gas purchase cost is decreased by 9.1 %. It can be seen that the introduction of ladder-type carbon trading mechanism can achieve low-carbon operation of the system and effectively alleviate environmental pollution.

The research content of this paper still has some shortcomings, such as not considering the time-of-use gas price. In the follow-up work, we can consider the time-of-use gas price and further study the impact of carbon trading base price, carbon emission interval length and carbon trading price increase on carbon trading costs and carbon emissions in carbon trading mechanism.

## CRedit authorship contribution statement

**Peihong Yang:** Methodology, Formal analysis, Writing – original draft. **Hui Jiang:** Methodology, Writing – review & editing, Data curation. **Chunming Liu:** Project administration, Resources. **Lan Kang:** Visualization, Funding acquisition. **Chunling Wang:** Writing – review & editing.

## Declaration of Competing Interest

The authors declare that they have no known competing financial interests or personal relationships that could have appeared to influence the work reported in this paper.

## Data availability

Data will be made available on request.

## Acknowledgements

This work is supported by the science and technology planning project of the Inner Mongolia Autonomous Region under Grant No.2020GG0156, 2021GG0015, and 2022YFHH0027 & Program for Yong talents of Science and Technology in University of the Inner Mongolia Autonomous Region under Grant No.NJYT22055.

## References

- [1] You C, Kim J. Optimal design and global sensitivity analysis of a 100% renewable energy sources based smart energy network for electrified and hydrogen cities. *Energy Convers Manage* 2020;223:113252. <https://doi.org/10.1016/j.enconman.2020.113252>.
- [2] Wang S, Meng Z, Yuan S. IEC 61970 standard based common information model extension of electricity-gas-heat integrated energy system. *Int J Electr Power Energy Syst* 2020;118:105846. <https://doi.org/10.1016/j.ijepes.2020.105846>.
- [3] Li J, Huang Y, Zhu M. Gradient descent iterative method for energy flow of integrated energy system considering multiple modes of compressors. *Energy Convers Manage* 2020. <https://doi.org/10.1016/j.enconman.2020.112534>.
- [4] Wang Z, Hu J, Liu B. Stochastic optimal dispatching strategy of electricity-hydrogen-gas-heat integrated energy system based on improved spectral clustering method. *Int J Electr Power Energy Syst* 2020;126:106495. <https://doi.org/10.1016/j.ijepes.2020.106495>.
- [5] Li J, Zhu M, Lu Y, Huang Y, Wu D. Review on optimal scheduling of integrated energy systems. *Power Syst Technol* 2021;45(6):2256–69. <https://doi.org/10.13335/j.1000-3673.pst.2021.0020>.
- [6] Bahrami S, Sheikhi A. From demand response in smart grid toward integrated demand response in smart energy hub. *IEEE Trans Smart Grid* 2015;7(2):650–8. <https://doi.org/10.1109/TSG.2015.2464374>.
- [7] Li P, Wang Z, Wang J, Yang W, Yin Y. Two-stage optimal operation of integrated energy system considering multiple uncertainties and integrated demand response. *Energy* 2021;225:120256. <https://doi.org/10.1016/j.energy.2021.120256>.
- [8] Qi B, Zheng S, Sun Y, Li B, Tian S, Shi KA. Model of incentive-based integrated demand response considering dynamic characteristics and multi-energy coupling effect of demand side. *Proc CSEE* 2022;42(5):1783–99. <https://doi.org/10.13334/j.0258-8013.psee.202351>.
- [9] Toolabi M, Soheily F, Sanei S, Akbari E, Khorramdel H, Ghadamyari M. Bi-level optimization of the integrated energy systems in the deregulated energy markets considering the prediction of uncertain parameters and price-based demand response program. *Energy Sci Eng* 2022;10(8):2772–93. <https://doi.org/10.1002/ese3.1166>.
- [10] Xu Z, Sun H, Guo Q. Review and prospect of integrated demand response. *Proc CSEE* 2018;38(24):7194–205. <https://doi.org/10.13334/j.0258-8013.psee.180893>.
- [11] Liu W, Huang Y, Li Z, Yang Y, Yi F. Optimal allocation for coupling device in an integrated energy system considering complex uncertainties of demand response. *Energy* 2020;198:117279. <https://doi.org/10.1016/j.energy.2020.117279>.
- [12] Yang Y, Yan G, Mu G. Bi-level decentralized control of electric heating loads considering wind power accommodation in real-time electricity market. *Int J Electr Power Energy Syst* 2022;135:107536. <https://doi.org/10.1016/j.ijepes.2021.107536>.
- [13] Sheikhi A, Bahrami S, Ranjbar AM. An autonomous demand response program for electricity and natural gas networks in smart energy hubs. *Energy* 2015;89:490–9. <https://doi.org/10.1016/j.energy.2015.05.109>.
- [14] Majidi M, Mohammadi-Ivatloo B, Anvari-Moghaddam A. Optimal robust operation of combined heat and power systems with demand response pro-grams. *Applied Therm Eng* 2019;149:1359–69. <https://doi.org/10.1016/j.applthermaleng.2018.12.088>.
- [15] Wang Y, Yang Y, Tang L, Sun W, Zhao H. A stochastic-CVaR optimization model for CCHP micro-grid operation with consideration of electricity market, wind power accommodation and multiple demand response programs. *Energies* 2019;12(20):3983. <https://doi.org/10.3390/en12203983>.
- [16] Shao C, Ding Y, Siano P, Lin Z. A framework for incorporating demand response of smart buildings into the integrated heat and electricity energy system. *IEEE Trans on Ind Electron* 2019;66(2):1465–75. <https://doi.org/10.1109/TIE.2017.2784393>.
- [17] Wang J, Zhong H, Ma Z, Xia Q, Kang C. Review and prospect of integrated demand response in the multi-energy system. *Appl Energy* 2017;202:772–82. <https://doi.org/10.1016/j.apenergy.2017.05.150>.
- [18] Nwulu NI, Xia X. Optimal dispatch for a microgrid incorporating renewables and demand response. *Renew Energy* 2017;101(3):16–28. <https://doi.org/10.1016/j.renene.2016.08.026>.
- [19] Wu H, Shahidehpour M, Khodayar M. Hourly demand response in day-ahead scheduling considering generating unit ramping cost. *IEEE Trans Power Syst* 2013;28(3):2446–54.
- [20] Kilkis S, Krajacic G, Duic N, Montorsi L, Wang Q, Rosen M, et al. Research frontiers in sustainable development of energy, water and environment systems in a time of climate crisis. *Energy Convers Manage* 2019;199:111938. <https://doi.org/10.1016/j.enconman.2019.111938>.
- [21] Yang J, Zhang N, Cheng Y, Kang C, Xia Q. Modeling the operation mechanism of combined P2G and gas-fired plant with CO2 recycling. *IEEE Trans Smart Grid* 2018;10(1):1111–21.

- [22] He L, Lu Z, Zhang J, Geng L, Zhao H, Li X. Low-carbon economic dispatch for electricity and natural gas systems considering carbon capture systems and power-to-gas. *Appl Energy* 2018. <https://doi.org/10.1016/j.apenergy.2018.04.119>.
- [23] Tan Q, Ding Y, Wei Y, He Q, Liu Y, Yao X. Research on Optimal Strategy of Carbon Emission Reduction for Thermal Power Enterprises Under Carbon Trading and Fuzzy Budget. *Power System Technology* 2019;43(10):3707-3715. [10.13335/j.1000-3673.pst.2019.1229](https://doi.org/10.13335/j.1000-3673.pst.2019.1229).
- [24] Yin A, Xu C, Ju L. A joint scheduling optimization model for wind power and energy storage systems considering carbon emissions trading and demand response. *Math Probl Eng* 2016. <https://doi.org/10.1155/2016/4070251>.
- [25] Wei Z, Zhang S, Sun G, Xu X, Chen S. Carbon trading based low-carbon economic operation for integrated electricity and natural gas energy system. *Autom Electr Power Syst* 2016;40(15):9–16. <https://doi.org/10.7500/AEPS20151109004>.
- [26] Cui Y, Zeng P, Wang Z, Wang M, Zang J. Low-carbon economic dispatch of an integrated electricity-gas-heat energy system considering stepped carbon trading. *Power Automat Equip* 2021;41(03):10–7. <https://doi.org/10.1016/j.energy.2021.120267>.
- [27] Wang Z, Shi Y, Tang Y, Meng X, Cao J. Low carbon economy operation and energy efficiency analysis of integrated energy systems considering LCA energy chain and carbon trading mechanism. *Proc CSEE* 2019;39(6):1614–26. <https://doi.org/10.13334/j.0258-8013.psee.180754>
- [28] Li Y, Tang W, Wu Q. Modified carbon trading based low-carbon economic dispatch strategy for integrated energy system with CCHP. Milan, Italy: IEEE Milan PowerTech 2019;2019:1-6. [10.1109/PTC.2019.8810482](https://doi.org/10.1109/PTC.2019.8810482).
- [29] Wang L, Dong H, Lin J, Zeng M. Multi-objective optimal scheduling model with IGDT method of integrated energy system considering ladder-type carbon trading mechanism. *Int J Electr Power Energy Syst* 2022;143:108386. <https://doi.org/10.1016/j.ijepes.2022.108386>.
- [30] Zhang N, Hu Z, Dai D, Dang S, Yao M, Zhou Y. Unit commitment model in Smart grid environment considering carbon emissions trading. *IEEE Trans Smart Grid* 2016;7(1):420–6. <https://doi.org/10.1109/TSG.2015.2401337>.
- [31] Cui Y, Zhang J, Wang Z, Wang T, Zhao Y. Day-ahead scheduling strategy of wind-PV-CSP hybrid power generation system by considering PDR. *Proc CSEE* 2020.
- [32] Wu J, Li X, Lin Y, Yan Y, Tu J. A PMV-based HVAC control strategy for office rooms subjected to solar radiation. *Building. Environ* 2020. <https://doi.org/10.1016/j.buildenv.2020.106863>.
- [33] Cheng J, Tan Z, Yue L. CCHP-SESS Bi-layer Optimal Configuration Considering Load Comprehensive Demand Response. *Power System Technology*.1-13[2022-08-24] [10.13335/j.1000-3673.pst.2022.0699](https://doi.org/10.13335/j.1000-3673.pst.2022.0699).
- [34] Zou Y, Yang L, Li J, Xiao L, Ye H, Lin Z. Robust optimal dispatch of micro-energy grid with multi-energy complementation of cooling heating power and natural gas. *Autom Electr Power Syst* 2019;43(14):65–72. <https://doi.org/10.7500/AEPS20181028004>.
- [35] Wang L, Shi Z, Dai W, Zhu L, Wang X, Cong H, et al. Two-stage stochastic planning for integrated energy systems accounting for carbon trading price uncertainty. *Int J Electr Power Energy Syst* 2022;143:108452. <https://doi.org/10.1016/j.ijepes.2022.108452>.
- [36] Lu S, Lou S, Wu Y, Yin X. Power system economic dispatch under low-carbon economy with carbon capture plants considered. *Iet Gener Transm Distrib* 2013;7(9):991–1001. <https://doi.org/10.1049/iet-gtd.2012.0590>.
- [37] Wang C, Hong B, Guo L, Zhang D, Liu W. A General Modeling Method for Optimal Dispatch of Combined Cooling, Heating and Power Microgrid. *Proceedings of the CSEE* 2013;33(31):26-33+3. [CNKI:SUN:ZGDC.0.2013-31-003](https://doi.org/10.13334/j.0258-8013.psee.13003).
- [38] Li Z, Chen L, Liu D, Chen F, Zheng T., Mei S. Subsidy Pricing Method for Stackelberg-game-based Energy Storage System. *High Voltage Engineering*, 46 (02) (2020), pp. 519-526. [10.13336/j.1003-6520.hve.20200131016](https://doi.org/10.13336/j.1003-6520.hve.20200131016).
- [39] Zhang T, Guo Y, Li Y, Yu L, Zhang J. Optimization scheduling of regional integrated energy systems based on electric-thermal-gas integrated demand response. *Power System Protect Control* 2021;49(1):52–61. <https://doi.org/10.19783/j.cnki.pspc.200167>.